

Available online at www.sciencedirect.com**ScienceDirect**

Procedia IUTAM 12 (2015) 193 – 203

**Procedia
IUTAM**www.elsevier.com/locate/procedia

IUTAM Symposium on Mechanics of Soft Active Materials

Controlled Sequential Shape Changing Components by 3D Printing of Shape Memory Polymer Multimaterials

Kai Yu^a, Alexander Ritchie^b, Yiqi Mao^a, Martin L. Dunn^c, H. Jerry Qi^{a*}^a*The George Woodruff School of Mechanical Engineering, Georgia Institute of Technology, Atlanta, GA 30332, USA*^b*School of Electrical and Computer Engineering, Georgia Institute of Technology, Atlanta, GA 30332, USA*^c*SUTD-MIT International Design Centre, Singapore University of Technology and Design, Singapore*

Abstract

In this paper, we demonstrate the feasibility of using 3D printing technique to create functional graded shape memory polymers (SMPs) with both spontaneous and sequential shape recovery abilities. The created SMP components, with properly assigned spatial variation of the thermodynamical property distribution, react rapidly to a thermal stimulus, and return to a specified configuration in a precisely controlled shape changing sequence. The use of the 3D printing technique enables a manufacturing routine with merits of easy implementation, large design freedom, and high printing resolution, which promises to advance immediate engineering applications for low-cost, rapid, and mass production.

© 2014 The Authors. Published by Elsevier B.V. This is an open access article under the CC BY-NC-ND license (<http://creativecommons.org/licenses/by-nc-nd/4.0/>).

Peer-review under responsibility of Konstantin Volokh and Mahmood Jabareen.

Keywords: Functionally gradient; shape memory polymers; 3D printing; 4D printing, multimaterial printing.

1. Introduction

Shape memory polymers (SMPs) are defined by the ability to recover their permanent shapes from one (or sometimes multiple¹⁻⁶) programmed temporary shape (s) when a proper stimulus is applied, such as temperature⁷⁻¹², magnetic fields¹³⁻¹⁷, light¹⁸⁻²³ and moisture^{24, 25} etc. This observed phenomenon is usually referred as shape memory (SM) effect in polymers. Since this type of smart materials could sense the environmental changes and then take reactions accordingly in a predetermined sequence, they are considered as a promising alternative for the future's

* Corresponding author. Tel.: 404-385-2457; fax: 404-385-8535.

E-mail address: qih@me.gatech.edu

spontaneous shape changing. Compared with shape memory alloys and ceramics, SMPs possess the advantages of high strain recovery²⁶, low density, low cost, easy shape programming procedure and easy control of recovery temperature. Besides, they are also chemically tunable to achieve biocompatibility and biodegradability, and hence gained extensive research interests recently in various areas such as medical, civil and industrial etc.²⁷⁻³⁰

While the spontaneous shape changing of SMPs has been well studied in the past few decades^{7, 28, 31-44}, the achievement of highly controlled sequential shape recovery is still a challenge. Currently, there are two main strategies in this realm: one involves exploring additional temporary shapes in a shape memory cycle, which can be realized either by tuning the shape memory transition temperature range^{5, 6, 45, 46} or tailoring discrete reversible transitions into a single SMP^{2-4, 47}. During the polymer free recovery, different temporary shapes can be reached in a predefined sequence upon changing the degree of environmental stimulus. The second strategy requires the polymer materials or structures to have spatially dependent compositions, microstructures or associated thermomechanical properties, namely the functional gradient within the polymer material⁴⁸⁻⁵⁰. When a right stimulus is applied, independent shape recoveries in each section of SMPs will be successively activated. The sequential fashion during the shape changing of SMPs can be manipulated by properly assigning material properties on each section. This new technique is expected to enable novel devices, sensors and actuators that can be widely applied in microsystem actuation components^{21, 51-53}, biomedical devices^{14, 42, 54} and aerospace deployable structures^{55, 56}.

There are many approaches to achieve functionally graded SMPs with sequential shape recovery properties. For example, by post-curing a pre-cured SMP on a surface with linear temperature gradient, Mather et al⁴⁸ successfully created functional SMPs where different sections of the material exhibit gradually increased glass transition temperature (T_g) and consequently react to different temperature degrees independently. Other synthetic methods include UV polymerization with patterned photo-filters⁵⁷, photo-degradation with a gradually removed mask⁵⁸, inter-diffusion of polymer bilayers⁵⁹ and co-extrusion with specially designed gradient distribution^{60, 61} etc. Though all these methods have their merits, they are generally inefficient in achieving a highly non-regular but precisely controlled material distribution within a single SMP. Additionally, their immediate engineering applications are limited where the manufacturing methods require ease of implementation and suitability for low-cost, rapid and mass production.

In this paper, we use the 3D printing technique⁶²⁻⁷¹ to create SMPs with both spontaneous and sequential shape changing properties. The manufacturing method involves direct 3D printing from a CAD file that specifies the details of material configuration and property distribution, which provides considerable design freedom and operation convenience during the creation of functionally graded SMPs. The polymer material we used is an epoxy based UV curable SMP, whose shape recovery is thermally triggered. By controlling the composition of printed materials, the glass transition temperatures of SMPs can be controlled to create a functional gradient. By properly specifying material properties in different sections, we experimentally demonstrated that the deformed SMP component can successfully return back to the original configuration in a predefined sequence, while the shape recovery in a SMP component without any property gradient will be either interfered or even failed in middle. By using this method, even complex three-dimension (3D) solids can be created with arbitrarily defined material distributions, which provide a potential route for precisely controlling the shape recovery profile and enabling the fabrication of devices with unprecedented multifunctional performance. This characteristic has been termed as 4D printing^{72, 73}.

2. Results and Discussion

2.1. Material Characterization

For the thermally responsive SMPs, the key to realize a sequential shape recovery is to introduce a tailored distribution of thermomechanical properties, allowing the specified material sections to independently react to temperature changes. In view of this, we start our experimental investigation by testing the thermomechanical properties of seven epoxy polymers (respectively labeled as SMP 1-7) that can be directly created by using the 3D multimaterial polymer printer (Objet Connex 260, Stratasys, Edina, MN, USA). The printing process works by depositing droplets of polymer ink at ~ 70 °C, wiping them into a smooth film, and then UV photopolymerizing the

film. Different polymer inks are respectively prepared by mixing two liquid monomers in specific ratios^{70, 71}. However, the exact chemical formula and composition of the commercial product is still unknown. During the 3D printing, we set the dimension of all SMP samples is as 15 mm×3 mm×0.6 mm in uniform for the following characterization tests.

After the SMP materials are printed, a dynamic mechanical analysis (DMA, TA Instruments, Model Q800) in uniaxial tension mode is performed to characterize their glass transition behavior. The SMP sample is firstly heated up to 100 °C on the DMA machine and stabilized for 20 minutes to reach thermal equilibrium, and then a preload of 1 KPa is applied. During the DMA experiment, the strain is oscillated at a frequency of 1 Hz with a peak-to-peak amplitude of 0.1% while the temperature is decreased from 100 °C to a given low temperature at a rate of 2 °C/min. Figure 1a and 1b show the storage modulus and $\tan \delta$ within the temperature variation range. It is seen the polymer modulus decreases linearly with temperature. The temperature corresponding to the peak of the $\tan \delta$ curve is taken to be the glass transition temperature T_g . Within the testing temperature range, it is seen that the storage modulus far below the T_g is about two orders of magnitude larger than that above T_g . The measured T_g of all the seven samples are summarized and plotted in Figure 1c. Considering the glass transition range of all the SMP materials, we select a temperature range from $T_L=10$ °C to $T_H=100$ °C in this paper to examine the polymer SME.

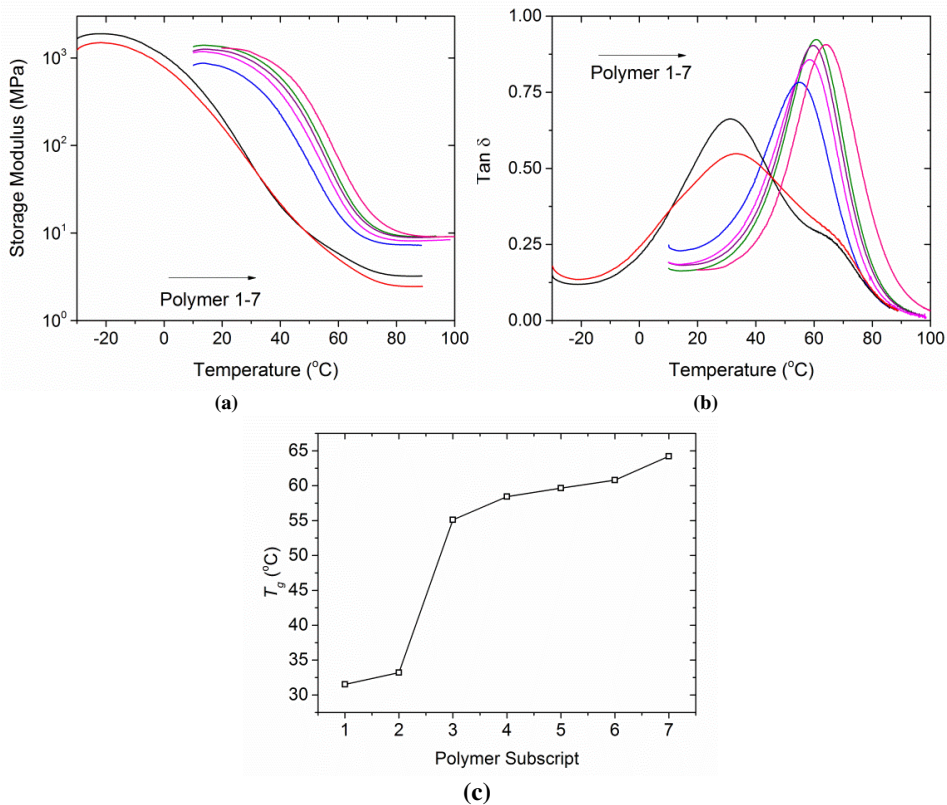


Figure 1. Thermodynamical properties of the SMP 1-7. (a) The temperature dependent storage modulus, (b) The temperature dependent $\tan \delta$ and (c) The summary of T_g

2.2. Sequential Shape Recovery in a Helical SMP Component

To demonstrate the sequential free shape recovery, we designed the following helical component in CAD software (see Figure 2), where rectangular plates are connected by hinge sections on the corner with a radius of

5mm. The thickness of the helical line is 0.8mm and the depth is 6mm. The clearance between neighbouring helical lines is 5mm. In the following study, each hinge section of the architecture will be assigned with different material properties based on the polymer list shown in Figure 1, and the helical structure will be deployed into a straight configuration during the programming step of the shape memory cycle. The material configuration shown in Figure 2 also represents the permanent shape that can be memorized by the printed SMP component.

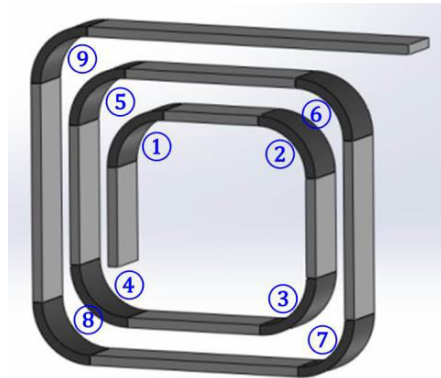


Figure 2. Schematic view of the helical SMP component

In the design, we assign the material distribution for the hinge section as: Polymer 1 with lowest T_g (~ 32 °C) is assigned to the two innermost hinges (Hinges 1 and 2); Polymer 7 with highest T_g (~ 65 °C) is assigned to the two outermost hinges (Hinges 8 and 9); the rest hinges (Hinges 3 and 7) are assigned with polymers (Polymer 2-6) with gradually increased T_g . It should be noted that the inhomogeneity of material distribution could be further refined into a micron scale based on the resolution of printer.

After printing, the free shape recovery of the created SMP component is exercised. We firstly heat the printed structure then deform it into a straight configuration in hot water with $T_H=100$ °C, which is above T_g of all the SMP material sections. Then the sample is moved into an environment with $T_L=10$ °C, where all the hinge sections are transferred to the glassy state and stiffen. After holding the sample at T_L for a time sufficient to equilibrate the strain (~ 10 min), we released the external loading and the component is able to fix the temporary programming shape.

To activate the free shape recovery of the SMP component, it is immersed into the hot water again with $T_r=100$ °C. The free shape recovery process is monitored by a video camera. Figure 3 shows the snapshots of the material configurations at different recovery time, which visually demonstrates a spontaneous and sequential SME in the created SMP component. Firstly, the material shows a rapid response to the thermal energy. Within 6.5s, the straight SMP component assembles into the original helical configuration as shown in Figure 2. The difference in T_g of hinge sections leads to a different shape recovery time. Since T_g of the three inner hinges is much lower than the outside ones, they firstly exhibit rotational shape recovery, and then the shape changing is successively triggered along the helical line. The rapid shape recovery of inner hinges leaves enough space for the coiling of out layers. Similar with the previous work about quantifying the shape recovery ratio, we define the bending shape recovery ratio (R_r) in this case as:

$$R_r = \frac{180^\circ - \theta(t)}{90^\circ}, \quad (1)$$

where $\theta(t)$ is the time dependent angle of each hinge section. The bending shape recovery ratio of each hinge of the SMP component is studied by image analysis and plotted as a function of recovery time in Figure 4. As shown in the figure, the first three hinges start the shape recovery within ~ 1 s after being immersed into the hot water, and the process is essentially finished within 3 seconds, while the last two hinges start to recover after 3 seconds and finish at 6.5s. The hierarchical shape recovery profiles of hinge section enable the successful sequential shape recovery in

the created SMP component without interruption.

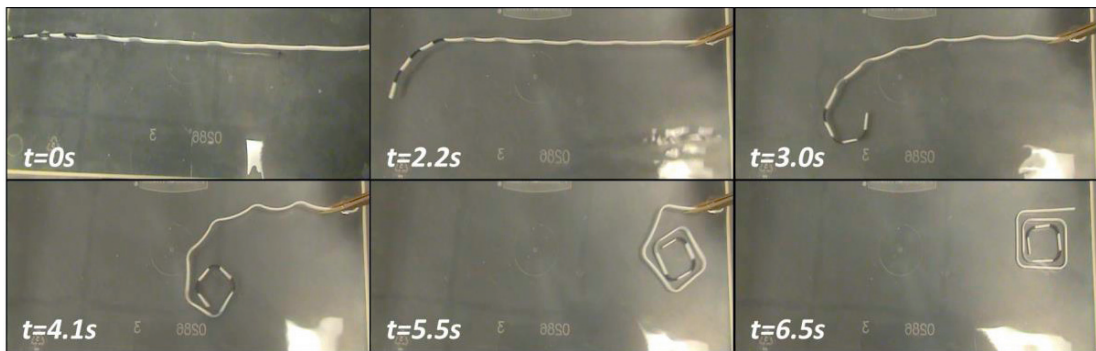


Figure 3. Series of photographs showing the spontaneous and sequential shape recovery process of the helical SMP component with graded hinge sections

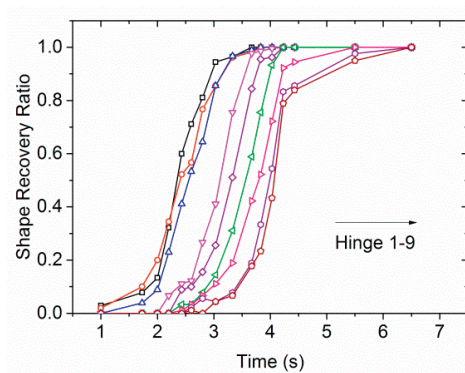


Figure 4. Shape recovery ratio of each hinge section plotted as a function of recovery time

As a controlling demonstration, we further tested the shape recovery behavior of SMP component without graded distribution of material properties. Another SMP component is manufactured with the same dimension and configuration as shown in Figure 1, where the hinge sections are using the same polymer material (polymer 3) with the $T_g \approx 55^\circ\text{C}$. After experiencing the same programming procedure as mentioned above, the SMP component is immersed in the hot water ($\sim 100^\circ\text{C}$) and the free recovery process is monitored and shown in Figure 5. Since the thermomechanical property is identical in each hinge section, the associated shape changing is induced almost simultaneously, which contrasts the first case with sequential shape recovery behavior. Before the full recovery of inner hinges, the outer layer of the SMP component coils back with equivalent speed. The interference of the shape recovery occurs at $\sim 8.5\text{s}$, where the frictional resistance due to contact prevent the SMP from recovery. In this manner, the shape recovery speed is dramatically decreased from 8.5s to 14.5s, and the shape changing finally stops at $\sim 14.5\text{s}$ with an incomplete shape recovery in the SMP component. The result confirms that the distribution of material property will impact the recovery manner of SMPs and a gradually increased T_g along the helical line is the key to realize the successful sequential shape recovery of the created SMP component.

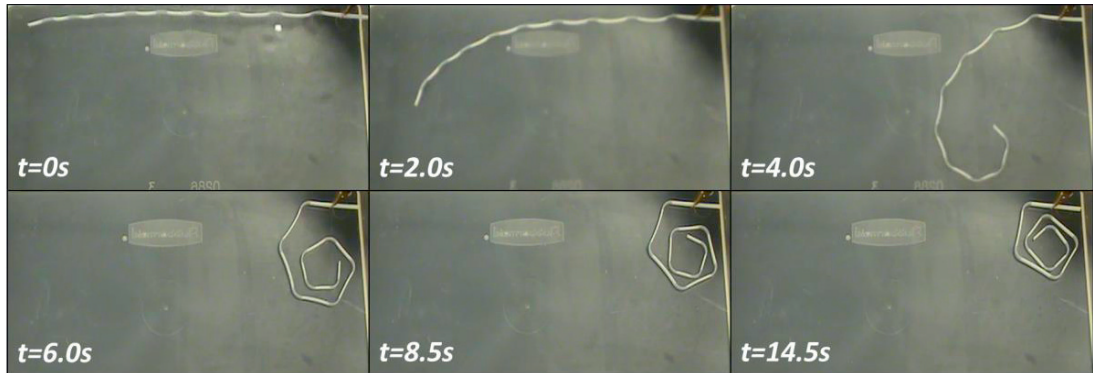


Figure 5. Series of photographs showing the shape recovery process of the helical SMP component with uniform hinge section

2.3. Sequential Shape Recovery in an Inter-locking SMP Component

The sequential shape changing will not only benefit us with smooth shape recovery as shown above, but also the realization of full recovery in SMP components manufactured in special configurations, which requires highly controlled sequence during the shape recovery of different material sections. To demonstrate this, a SMP component with interlocking feature is created and schematically shown in Figure 6. Two holes with different dimensions are designed on the ending plate, which allows the other end bend over through them to form the locking configuration. The thickness of SMP component is 0.6mm (0.8mm for the plate with holes) and the depth is 6mm. Five hinge sections (with a radius of 5mm in uniform) rested on the corner will be assigned with different SMP materials. For a representative case, Hinges 1-5 will be assigned with Polymer 2, 2, 3, 6 and 6 respectively.

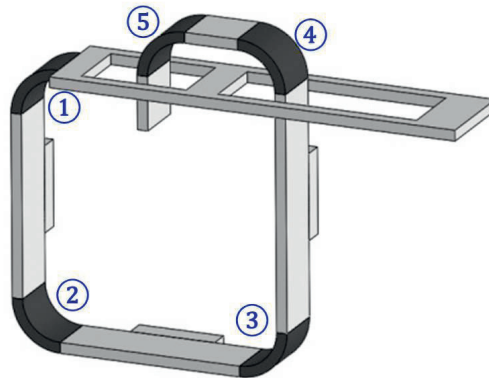


Figure 6. Schematic view of the interlocking SMP component

At the temperature of 100 °C, the SMP component is firstly deployed into a straight line, namely an unlocked configuration. Then it is cooled back to 10°C and stabilized for 30min after removing the external load. After the programming step, the SMP component is immersed in the hot water (~100°C) and the free recovery process is monitored both of the top and side view, as shown in the snapshots of Figure 7. With the specified material properties on each hinge section, the SMP component is seen to return into the original interlocking configuration at ~14.2s. The shape changing process reveals that to successfully recover into the original interlocking configuration, the sequential shape recovery of the SMP component should satisfy two requirements: Firstly, the shape recovery of the first two hinges should be the faster than the rest ones so that the two end sides could hit each other with a right position and angle. Secondly, the shape recovery of the last two hinges should be slower to guarantee the active locking side could pass through the two holes successively.

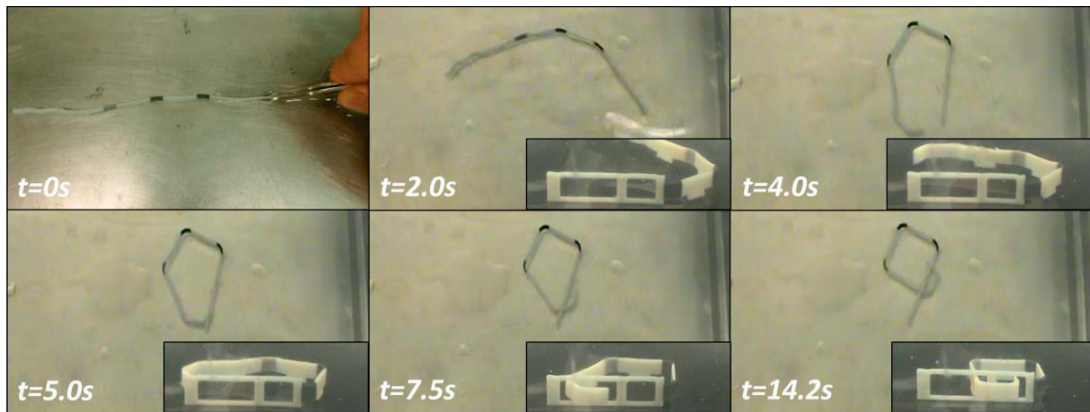


Figure 7. Series of photographs showing the spontaneous and sequential shape recovery process of the interlocking SMP component with graded distribution of hinge section

These two qualitative criteria could be satisfied by properly arranging the material properties on each hinge section. A change in the properties distribution could lead to a change of recovery manner and potentially a failure in recovering the interlocking configuration of the SMP component. Figure 8 shows final shape recovery of two SMP components with different material assignment. In Figure 8a, the sequence of material distribution is reversed, namely Hinges 1-5 are assigned with Polymer 6, 6, 3, 2 and 2 respectively, while in Figure 8b, all the hinge sections are using the same SMP material (Polymer 3). In both two cases, the last two hinges achieved a nearly full shape recovery before the active locking side reaching the passive locking side, which leads to a stuck in front of the first hole.

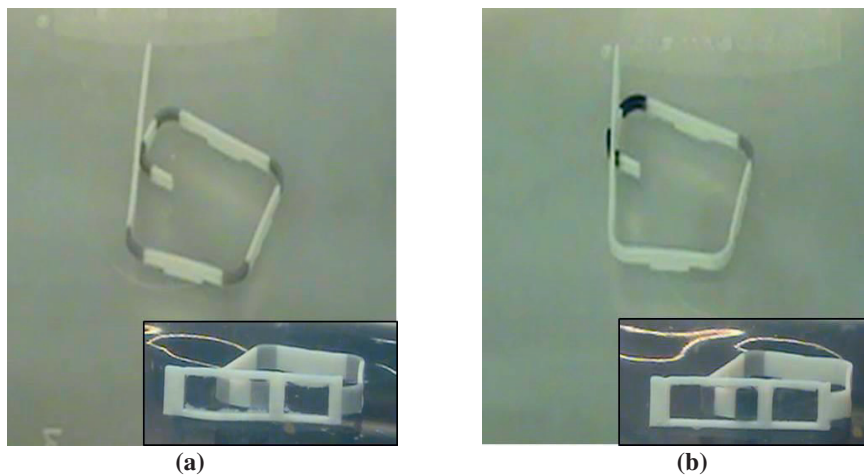


Figure 8. The final recovered shape of two types of interlocking SMP components. (a) All the hinge sections are using the same material. (b) The sequence of material distribution is reversed compared with the material in Figure 7.

3. Conclusion

In this paper, we experimentally demonstrated the feasibility of using 3D printing to create SMP material with functional gradient. Both the helical and self-interlocking SMP components featured here show not only the reliability of spontaneous shape recovery, but also a precisely controlled shape changing sequence that can be utilized to reach the specified material configurations smoothly and successfully. This precision, achieved by a selection of priority distribution of material properties, makes possible the implementation of the polymer shape memory effect in an extremely wide array of objects and applications yet to be realized, such as structures involving

complex deformation permutations, and the development of practical and versatile SMP solids able to self-adjust and self-reinforce to cope uniquely with different environmental conditions etc. By using three-dimensional printing technique, the SMP structures with both spontaneous and sequential properties could be directly created with large design freedom and high resolution of material properties distribution. Besides, the manufacturing route could be easily implemented and potential for immediate engineering applications for low-cost, rapid and mass production.

Acknowledgements

We gratefully acknowledge the support of an AFOSR grant (FA9550-13-1-0088; Dr. B.-L. “Les” Lee, Program Manager). HJQ acknowledge the support of the NSF award (CMMI-1404621 and EFRI- 1435452). MLD acknowledges support from the MOE of Singapore and the SUTD-MIT International Design Centre.

References

1. Pretsch, T., *Triple-shape properties of a thermoresponsive poly(ester urethane)*. Smart Materials & Structures, 2010. **19**(1).
2. Behl, M., I. Bellin, S. Kelch, W. Wagermaier, and A. Lendlein, *One-Step Process for Creating Triple-Shape Capability of AB Polymer Networks*. Advanced Functional Materials, 2009. **19**(1): p. 102-108.
3. Bellin, I., S. Kelch, and A. Lendlein, *Dual-shape properties of triple-shape polymer networks with crystallizable network segments and grafted side chains*. Journal of Materials Chemistry, 2007. **17**(28): p. 2885-2891.
4. Luo, X.F. and P.T. Mather, *Triple-Shape Polymeric Composites (TSPCs)*. Advanced Functional Materials, 2010. **20**(16): p. 2649-2656.
5. Xie, T., *Tunable polymer multi-shape memory effect*. Nature, 2010. **464**(7286): p. 267-270.
6. Li, J.J. and T. Xie, *Significant Impact of Thermo-Mechanical Conditions on Polymer Triple-Shape Memory Effect*. Macromolecules, 2011. **44**(1): p. 175-180.
7. Lendlein, A. and S. Kelch, *Shape-memory polymers*. Angew Chem Int Ed Engl, 2002. **41**(12): p. 2035-57.
8. Liu, C., H. Qin, and P.T. Mather, *Review of progress in shape-memory polymers*. Journal of Materials Chemistry, 2007. **17**(16): p. 1543-1558.
9. Chung, T., A. Rorno-Urbe, and P.T. Mather, *Two-way reversible shape memory in a semicrystalline network*. Macromolecules, 2008. **41**(1): p. 184-192.
10. Gall, K., C.M. Yakacki, Y.P. Liu, R. Shandas, N. Willett, and K.S. Anseth, *Thermomechanics of the shape memory effect in polymers for biomedical applications*. Journal of Biomedical Materials Research Part A, 2005. **73A**(3): p. 339-348.
11. Mather, P.T., X.F. Luo, and I.A. Rousseau, *Shape Memory Polymer Research*. Annual Review of Materials Research, 2009. **39**: p. 445-471.
12. Yu, K., Z.C. Zhang, Y.J. Liu, and J.S. Leng, *Carbon nanotube chains in a shape memory polymer/carbon black composite: To significantly reduce the electrical resistivity*. Applied Physics Letters, 2011. **98**(7).
13. Mohr, R., K. Kratz, T. Weigel, M. Lucka-Gabor, M. Moneke, and A. Lendlein, *Initiation of shape-memory effect by inductive heating of magnetic nanoparticles in thermoplastic polymers*. Proceedings of the National Academy of Sciences of the United States of America, 2006. **103**(10): p. 3540-3545.
14. Buckley, P.R., G.H. McKinley, T.S. Wilson, W. Small, W.J. Benett, J.P. Bearinger, et al., *Inductively heated shape memory polymer for the magnetic actuation of medical devices*. Ieee Transactions on Biomedical Engineering, 2006. **53**(10): p. 2075-2083.
15. Schmidt, A.M., *Electromagnetic activation of shape memory polymer networks containing magnetic nanoparticles*. Macromolecular Rapid Communications, 2006. **27**(14): p. 1168-1172.
16. He, Z.W., N. Satarkar, T. Xie, Y.T. Cheng, and J.Z. Hilt, *Remote Controlled Multishape Polymer Nanocomposites with Selective Radiofrequency Actuations*. Advanced Materials, 2011. **23**(28): p. 3192-3196.
17. Kumar, U.N., K. Kratz, W. Wagermaier, M. Behl, and A. Lendlein, *Non-contact actuation of triple-shape effect in multiphase polymer network nanocomposites in alternating magnetic field*. Journal of Materials

- Chemistry, 2010. **20**(17): p. 3404-3415.
18. Jiang, H.Y., S. Kelch, and A. Lendlein, *Polymers move in response to light*. *Advanced Materials*, 2006. **18**(11): p. 1471-1475.
 19. Koerner, H., G. Price, N.A. Pearce, M. Alexander, and R.A. Vaia, *Remotely actuated polymer nanocomposites - stress-recovery of carbon-nanotube-filled thermoplastic elastomers*. *Nature Materials*, 2004. **3**(2): p. 115-120.
 20. Lendlein, A., H.Y. Jiang, O. Junger, and R. Langer, *Light-induced shape-memory polymers*. *Nature*, 2005. **434**(7035): p. 879-882.
 21. Li, M.H., P. Keller, B. Li, X.G. Wang, and M. Brunet, *Light-driven side-on nematic elastomer actuators*. *Advanced Materials*, 2003. **15**(7-8): p. 569-572.
 22. Scott, T.F., R.B. Draughon, and C.N. Bowman, *Actuation in crosslinked polymers via photoinduced stress relaxation*. *Advanced Materials*, 2006. **18**(16): p. 2128-+.
 23. Scott, T.F., A.D. Schneider, W.D. Cook, and C.N. Bowman, *Photoinduced plasticity in cross-linked polymers*. *Science*, 2005. **308**(5728): p. 1615-1617.
 24. Huang, W.M., B. Yang, L. An, C. Li, and Y.S. Chan, *Water-driven programmable polyurethane shape memory polymer: Demonstration and mechanism*. *Applied Physics Letters*, 2005. **86**(11): p. -.
 25. Jung, Y.C., H.H. So, and J.W. Cho, *Water-responsive shape memory polyurethane block copolymer modified with polyhedral oligomeric silsesquioxane*. *Journal of Macromolecular Science Part B-Physics*, 2006. **45**(4): p. 453-461.
 26. Wei, Z.G., R. Sandstrom, and S. Miyazaki, *Shape-memory materials and hybrid composites for smart systems - Part I Shape-memory materials*. *Journal of Materials Science*, 1998. **33**(15): p. 3743-3762.
 27. Yakacki, C.M., R. Shandas, C. Lanning, B. Rech, A. Eckstein, and K. Gall, *Unconstrained recovery characterization of shape-memory polymer networks for cardiovascular applications*. *Biomaterials*, 2007. **28**(14): p. 2255-2263.
 28. Lendlein, A. and S. Kelch, *Shape-memory polymers as stimuli-sensitive implant materials*. *Clinical Hemorheology and Microcirculation*, 2005. **32**(2): p. 105-116.
 29. Liu, Y.P., K. Gall, M.L. Dunn, A.R. Greenberg, and J. Diani, *Thermomechanics of shape memory polymers: Uniaxial experiments and constitutive modeling*. *International Journal of Plasticity*, 2006. **22**(2): p. 279-313.
 30. Liu, Y.P., K. Gall, M.L. Dunn, and P. McCluskey, *Thermomechanics of shape memory polymer nanocomposites*. *Mechanics of Materials*, 2004. **36**(10): p. 929-940.
 31. Yu, K., Q. Ge, and H.J. Qi, *Reduced time as a unified parameter determining fixity and free recovery of shape memory polymers*. *Nature communications*, 2014. **5**: p. 3066.
 32. Yu, K., Q. Ge, and H.J. Qi, *Effects of stretch induced softening on the free recovery behavior of shape memory polymer composites*. *Polymer* (available on line), 2014.
 33. Yu, K., A.J.W. McClung, G.P. Tandon, J.W. Baur, and H.J. Qi, *A thermomechanical constitutive model for an epoxy based shape memory polymer and its parameter identifications*. *Mechanics of Time-Dependent Materials*, 2014. **18**(2): p. 453-474.
 34. Yu, K., D.M. Phillips, J.W. Baur, and H.J. Qi, *Analysis of shape-memory polymer composites with embedded microvascular system for fast thermal response*. *Journal of Composite Materials*, 2014: p. 0021998314540194.
 35. Yu, K., K.K. Westbrook, P.H. Kao, J. Leng, and H.J. Qi, *Design considerations for shape memory polymer composites with magnetic particles*. *Journal of Composite Materials*, 2013. **47**(1): p. 51-63.
 36. Yu, K., Z. Zhang, Y. Liu, and J. Leng, *Carbon nanotube chains in a shape memory polymer/carbon black composite: To significantly reduce the electrical resistivity*. *Applied Physics Letters*, 2011. **98**(7): p. 074102-074102-3.
 37. Yu, K., Y. Liu, and J. Leng, *Shape memory polymer/CNT composite and its microwave induced shape memory behavior*. *RSC Adv.*, 2013.
 38. Yu, K., Y. Liu, Y. Liu, H.-X. Peng, and J. Leng, *Mechanical and shape recovery properties of shape memory polymer composite embedded with cup-stacked carbon nanotubes*. *Journal of Intelligent Material Systems and Structures*, 2013: p. 1045389X13504475.
 39. Yu, K., Y.J. Liu, and J.S. Leng, *Conductive Shape Memory Polymer Composite Incorporated with Hybrid Fillers: Electrical, Mechanical, and Shape Memory Properties*. *Journal of Intelligent Material Systems and*

- Structures, 2011. **22**(4): p. 369-379.
40. Diani, J., P. Gilormini, C. Fredy, and I. Rousseau, *Predicting thermal shape memory of crosslinked polymer networks from linear viscoelasticity* International Journal of Solids and Structure, 2012. **49**(5): p. 793-799.
 41. Ge Q., Yu K. , Ding Y.F., and Qi J.H., *Prediction of temperature-dependent free recovery behaviors of amorphous shape memory polymers*. Soft Matter, 2012. **8**: p. 11098-11105.
 42. Lendlein, A. and R. Langer, *Biodegradable, elastic shape-memory polymers for potential biomedical applications*. Science, 2002. **296**(5573): p. 1673-1676.
 43. Nguyen, T.D., H.J. Qi, F. Castro, and K.N. Long, *A thermoviscoelastic model for amorphous shape memory polymers: Incorporating structural and stress relaxation* Journal of the Mechanics and Physics of Solids, 2008. **56** (9): p. 2792-2814
 44. Westbrook, K.K., P.H. Kao, F. Castro, Y.F. Ding, and H.J. Qi, *A 3D finite deformation constitutive model for amorphous shape memory polymers: A multi-branch modeling approach for nonequilibrium relaxation processes*. Mechanics of Materials, 2011. **43**(12): p. 853-869.
 45. Xie, T., K.A. Page, and S.A. Eastman, *Strain-Based Temperature Memory Effect for Nafion and Its Molecular Origins*. Advanced Functional Materials, 2011. **21**(11): p. 2057-2066.
 46. Yu, K., T. Xie, J. Leng, Y. Ding, and H.J. Qi, *Mechanisms of multi-shape memory effects and associated energy release in shape memory polymers*. Soft Matter, 2012. **8**(20): p. 5687-5695.
 47. Ge, Q., X.F. Luo, C.B. Iversen, P.T. Mather, M.L. Dunn, and H.J. Qi, *Mechanisms of triple-shape polymeric composites due to dual thermal transitions*. Soft Matter, 2013. **9**(7): p. 2212-2223.
 48. DiOrio, A.M., X.F. Luo, K.M. Lee, and P.T. Mather, *A functionally graded shape memory polymer*. Soft Matter, 2011. **7**(1): p. 68-74.
 49. Yang, B., W.M. Huang, C. Li, and J.H. Chor, *Effects of moisture on the glass transition temperature of polyurethane shape memory polymer filled with nano-carbon powder*. European Polymer Journal 2005. **41**(5): p. 1123-1128.
 50. Yang, B., W.M. Huang, C. Li, and L. Li, *Effects of moisture on the thermomechanical properties of a polyurethane shape memory polymer*. Polymer, 2006. **47**(4): p. 1348-1356.
 51. Chen, Z. and X.B. Tan, *A Control-Oriented and Physics-Based Model for Ionic Polymer-Metal Composite Actuators*. Ieee-Asme Transactions on Mechatronics, 2008. **13**(5): p. 519-529.
 52. Cho, J.W., J.W. Kim, Y.C. Jung, and N.S. Goo, *Electroactive shape-memory polyurethane composites incorporating carbon nanotubes*. Macromolecular Rapid Communications, 2005. **26**(5): p. 412-416.
 53. Lu, H., K. Yu, Y. Liu, and J. Leng, *Sensing and actuating capabilities of a shape memory polymer composite integrated with hybrid filler*. Smart Materials and Structures, 2010. **19**(6): p. 065014.
 54. Gomes, M.E. and R.L. Reis, *Biodegradable polymers and composites in biomedical applications: from catgut to tissue engineering - Part 1 - Available systems and their properties*. International Materials Reviews, 2004. **49**(5): p. 261-273.
 55. Yu, K., S. Sun, L. Liu, Z. Zhang, Y. Liu, and J. Leng. *Novel deployable morphing wing based on SMP composite*. in *Second International Conference on Smart Materials and Nanotechnology in Engineering*. 2009. International Society for Optics and Photonics.
 56. Yu, K., W. Yin, S. Sun, Y. Liu, and J. Leng. *Design and analysis of morphing wing based on SMP composite*. in *The 16th International Symposium on: Smart Structures and Materials & Nondestructive Evaluation and Health Monitoring*. 2009. International Society for Optics and Photonics.
 57. Wong, J.Y., A. Velasco, P. Rajagopalan, and Q. Pham, *Directed movement of vascular smooth muscle cells on gradient-compliant hydrogels*. Langmuir, 2003. **19**(5): p. 1908-1913.
 58. Yao, X.F., D.L. Liu, and H.Y. Yeh, *Mechanical properties and gradient variations of polymers under ultraviolet radiation*. Journal of Applied Polymer Science, 2007. **106**(5): p. 3253-3258.
 59. Hexig, B., H. Alata, N. Asakawa, and Y. Inoue, *Novel biodegradable poly(butylene succinate)/poly(ethylene oxide) blend film with compositional and spherulite-size gradients*. Journal of Polymer Science Part B-Polymer Physics, 2005. **43**(4): p. 368-377.
 60. Zhu, Y.B., N.Y. Ning, Y. Sun, Q. Zhang, and Q. Fu, *A new technique for preparing a filled type of polymeric gradient material*. Macromolecular Materials and Engineering, 2006. **291**(11): p. 1388-1396.
 61. Wen, B.Y., G. Wu, and J. Yu, *A flat polymeric gradient material: preparation, structure and property*. Polymer, 2004. **45**(10): p. 3359-3365.

62. Bogue, R., *3D printing: the dawn of a new era in manufacturing?* Assembly Automation, 2013. **33**(4): p. 307-311.
63. Bose, S., S. Vahabzadeh, and A. Bandyopadhyay, *Bone tissue engineering using 3D printing*. Materials Today, 2013. **16**(12): p. 496-504.
64. Brecht, J.F., *New Life for 3D Printing*. R&D Magazine, 2012. **54**(2): p. 12-13.
65. Campbell, T.A. and O.S. Ivanova, *3D printing of multifunctional nanocomposites*. Nano Today, 2013. **8**(2): p. 119-120.
66. Hockaday, L.A., K.H. Kang, N.W. Colangelo, P.Y.C. Cheung, B. Duan, E. Malone, et al., *Rapid 3D printing of anatomically accurate and mechanically heterogeneous aortic valve hydrogel scaffolds*. Biofabrication, 2012. **4**(3).
67. Martinez, E., L.E. Murr, K.N. Amato, J. Hernandez, P.W. Shindo, S.M. Gaytan, et al., *3d Microstructural Architectures for Metal and Alloy Components Fabricated by 3d Printing/Additive Manufacturing Technologies*. Proceedings of the 1st International Conference on 3d Materials Science, 2012: p. 73-78.
68. Richards, D.J., Y. Tan, J. Jia, H. Yao, and Y. Mei, *3D Printing for Tissue Engineering*. Israel Journal of Chemistry, 2013. **53**(9-10): p. 805-814.
69. Zhang, J.H., *3D Printing Technology-A New Mode of Computer-aided Style Design in This New Age*. Industrial Instrumentation and Control Systems Ii, Pts 1-3, 2013. **336-338**: p. 1383-1386.
70. Ge, Q., H. J. Qi, and M.L. Dunn, *Active materials by four-dimension printing*. Applied Physics Letters, 2013. **103**: p. 131901.
71. Ge, Q., C. Dunn, H.J. Qi, and M.L. Dunn, *Active Origami by 4D Printing*. Smart Materials and Structures (In press), 2014.
72. Tibbitts, S., *Design to Self-Assembly*. Architectural Design, 2012. **82**(2): p. 68-73.
73. Tibbitts, S. and K. Cheun, *Programmable materials for architectural assembly and automation*. Assembly Automation, 2012. **32**(3): p. 216-225.